Metal-Insulator Transition in $SrTiO_{3-x}$ Thin Films Induced by Frozen-Out Carriers

Z. Q. Liu,[1,2] D. P. Leusink,[1,2,4] X. Wang,[1,2] W. M. Lü,[1,3] K. Gopinadhan,[1,3] A. Annadi,[1,2] Y. L. Zhao,[1,2] X. H. Huang,[1,3] S. W. Zeng,[1,2] Z. Huang,[1] A. Srivastava,[1,2] S. Dhar,[1,3] T. Venkatesan,[1,2,3] and Ariando[1,2,*]

[1]*NUSNNI-Nanocore, National University of Singapore, 117542 Singapore*
[2]*Department of Physics, National University of Singapore, 117542 Singapore*
[3]*Department of Electrical and Computer Engineering, National University of Singapore, 117542 Singapore*
[4]*Faculty of Science and Technology and* MESA$^+$ *Institute for Nanotechnology, University of Twente, 7500 AE Enschede, The Netherlands*

(Received 20 April 2011; published 28 September 2011)

We report optical, electrical and magnetotransport properties of oxygen deficient $SrTiO_3$ ($SrTiO_{3-x}$) thin films fabricated by pulsed laser deposition technique. The oxygen vacancies (O_{vac}) in the thin film are expected to be uniform. By comparing its electrical properties to those of bulk $SrTiO_{3-x}$, it was found that O_{vac} in bulk $SrTiO_{3-x}$ is far from uniform over the whole material. The metal-insulator transition (MIT) observed in the $SrTiO_{3-x}$ film was found to be induced by the carrier freeze-out effect. The low temperature frozen state can be reexcited by Joule heating, electric and intriguingly magnetic field.

DOI: 10.1103/PhysRevLett.107.146802 PACS numbers: 73.40.Rw, 73.50.Gr, 73.20.Hb

Like Silicon in the semiconductor technology, $SrTiO_3$ (STO) is the most used substrate in oxide electronics because of its large dielectric constant [1], the close lattice match to a wide range of other perovskite oxides and its excellent thermal and chemical stabilities. Recently, two-dimensional electron gas [2,3] and electronic phase separation [4] have been demonstrated to emerge at the bare STO surface. Understanding the electronic and magnetic properties of STO under different oxidation states and external excitations is therefore very crucial to reveal the origin of these emerging phenomena and to use STO in devices. STO is a typical nonpolar band insulator with an indirect band gap of ~3.27 eV [5], but $SrTiO_{3-x}$ can show a metallic phase with a flexible tunability in electrical conductivity depending on the concentration of O_{vac}. $SrTiO_{3-x}$ is also the first oxide-based superconductor [6] with $T_c \sim 0.1$–0.6 K [7]. Shubnikov–de Haas (SdH) oscillations [8] have also been observed under usual laboratorial magnetic fields due to the high mobility [9] of free electrons. As a result of the large effective mass of the electrons at the bottom of the conduction band, $SrTiO_{3-x}$ possesses a large Seebeck coefficient of ~890 μV/K at room temperature (RT) [10], thus being a focus point in solid state thermoelectrics too.

Although there are so many interesting phenomena in $SrTiO_{3-x}$, the inhomogeneity of O_{vac} obtained by reducing bulk single crystals in vacuum and at high temperature is always an issue [6–11]; that is because the diffusion process of oxygen ions is usually proportional to the square root of time and the diffusion coefficient of oxygen ions in STO is small, $\sim 10^{-10}$ cm^2/s at 950 °C [12]. Taking 1 h as the annealing time at 950 °C, the diffusion length $l = \sqrt{Dt}$ of oxygen ions in single crystal STO will be ~6 μm, where D is the diffusion coefficient and t is the annealing time. Tufte and Chapman [9] found that the $SrTiO_{3-x}$ begins to reoxidize from ~500 K. Frederikse *et al.* [8] observed SdH oscillations in $SrTiO_{3-x}$ samples, which theoretically and also experimentally prefer to appear in a high mobility two-dimensional electron system [13]. These observations suggest that the O_{vac} may mostly exist near the surface rather than uniformly over the whole bulk material. Therefore, the values of some physical quantities [6–11] like resistivity (ρ) and carrier density (n), which were derived from the thickness of the whole bulk sample, would be of dubious validity. On the other hand, the intrinsic properties of the material are closely related to these physical parameters. For example, the superconducting T_c of $SrTiO_{3-x}$ apparently depends on n [7,11]. Additionally, the inhomogeneities could generate significant influence on electrical and galvanomagnetic measurements, and could even give rise to intriguing quantum effect—linear magnetic field dependence of the transverse magnetoresistance (MR) [14,15].

Here we report the metal-insulator transition (MIT) observed in $SrTiO_{3-x}$ thin film, in which O_{vac} are expected to uniformly distribute. As a highly interesting subject in condensed matter physics, MIT has various intriguing mechanisms [16]. However the MIT observed here is ascribed to the deionization effect of O_{vac} with decreasing temperature, which serve as doubly charged donor centers to make $SrTiO_{3-x}$ metallic at high temperatures. Both ρ and n are significantly different from the ones of the bulk samples with the carrier freeze-out phenomenon [9]. The frozen nonmetallic state can be reexcited by electric field and Joule heating. Surprisingly, it was found that the low temperature carrier freeze-out can also be suppressed by large magnetic fields, leading to negative MR.

Pulsed laser deposition technique was used to fabricate STO film from a single crystal STO target on a (100)-oriented $LaAlO_3$ (LAO) single crystal substrate (both sides

polished) under 6×10^{-3} Torr O_2 at 800 °C. During deposition, the fluence of laser energy was kept at 4 J/cm^2 and the repetition rate of the laser 4 Hz. To avoid the influence of the possible interface effect [13] and to keep the properties of the STO film akin to its bulk, a film with a thickness of ~2.6 μm was deposited.

The 3D topography atomic force microscope image of the as-deposited STO film [Fig. 1(a)] shows surface roughness of <6 nm with a root mean square value of ~0.541 nm for a 1×1 μm^2 area. The x-ray diffraction (Cu$K\alpha_1$ ray) pattern of the STO film is shown in Fig. 1(b). The adjacent double diffraction peaks of the film and the substrate for each order indicate the typical characteristic of epitaxial growth. LAO is an excellent substrate to study oxygen deficient films because it is fairly difficult to create O_{vac} inside. Although it is a polar material, the bulk LAO will experience surface reconstruction and thus its surface would be nonpolar. This was confirmed by our experiments, where STO layer-by-layer grown on fully LaO-terminated LAO was highly insulating, indicating no polar discontinuity at the interface.

The STO oxygen content was reduced by annealing the sample at 950 °C and ~1×10^{-7} Torr vacuum for 1 h. The transmittance spectrum [Fig. 1(c)] of the $SrTiO_{3-x}$ film was measured using ultraviolet-visible (UV) spectroscopy from 240 to 1600 nm. The absorption edge is ~380 nm, corresponding to the band gap of STO. This suggests that after vacuum annealing the lattice structure of the $SrTiO_{3-x}$ film is still well standing. The spectrum displays an interference pattern with relatively high transmittance above 380 nm, which pertains to a scenario where the thick and highly smooth $SrTiO_{3-x}$ film serves as a Fabry-Perot interferometer. So the transmittance will show peaks when the wavelength λ of the normal incident optical wave meets the condition $2m(\lambda)d = k\lambda$, where $m(\lambda)$ is the refractive index as a function of wavelength due to the strong dispersion [17], d is the film thickness, and k is the order of the fringe. Equivalently, the transmittance will periodically oscillate with $m(\lambda)/\lambda$ at a period of $1/2d$. To estimate the film thickness from the oscillations, a refractive index of 2.0516 was used [18]. Thus if the transmittance data of the wavelength from 380 to 1600 nm are plotted versus $1/\lambda$ as shown in the inset of Fig. 1(c), the average period of the oscillations in $1/\lambda$ will be $1/2md$. The fitted average period is 9.66384×10^{-5} nm^{-1} and therefore the derived thickness is 2524 nm. The value is consistent with the directly measured one but slightly smaller since the intrinsic refractive index should be smaller than that of a usual STO film due to the O_{vac} [19].

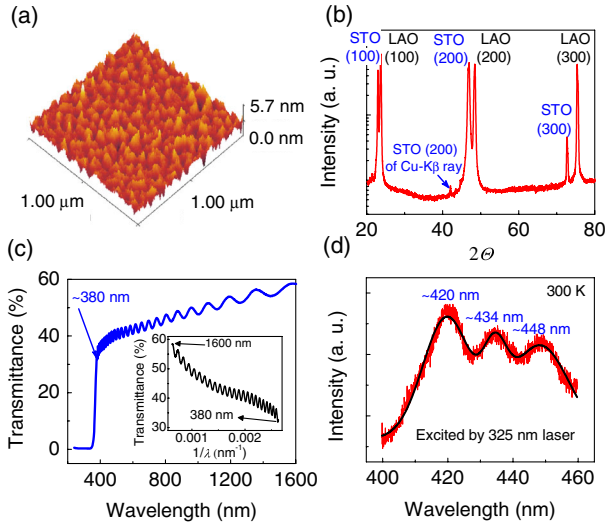

FIG. 1 (color online). (a) 3D atomic force microscope image of a 1×1 μm^2 area of the STO film. (b) X-ray diffraction of as-grown STO film on LAO substrate. (c) RT ultraviolet-visible-infrared spectroscopy of the $SrTiO_{3-x}$ film (obtained by annealing in ~1×10^{-7} Torr vacuum at 950 °C for 1 h) from 240 to 1600 nm. (Inset) The transmittance data versus the reciprocal of the wavelength from 380 to 1600 nm. (d) RT photoluminescence spectroscopy of the $SrTiO_{3-x}$ film between 400 and 460 nm.

The optical absorption of free electrons generated from O_{vac} is not seen in the UV spectroscopy, which typically leads to a decrease in transmittance especially in the long wavelength region and is likely buried by the strong interference. However, the multiple photoluminescence (PL) emission peaks mostly from the O_{vac} [20] can be clearly seen [Fig. 1(d)]. The three PL peaks correspond to the energy intervals 2.95, 2.86 and 2.76 eV, respectively.

The transport properties of the $SrTiO_{3-x}$ film were measured by a Quantum Design PPMS machine. Aluminum wires were used through wire bonding for contacts. The temperature dependence of resistivity (ρ-T) measured by 10 μA is shown on a logarithmic scale in Fig. 2(a). There is no observable difference between the cooling down and warming up ρ-T curves. The ρ-T curves reveal a clear MIT at ~78 K: at $T > 78$ K, ρ is small and shows metallic behavior; at $T < 78$ K, ρ increases with decreasing temperature and at 2 K reaches around 6 times of that at RT. Figure 2(b) shows that n decreases by an order of magnitude when decreasing the temperature from 300 to 10 K. These are the characteristics of a carrier

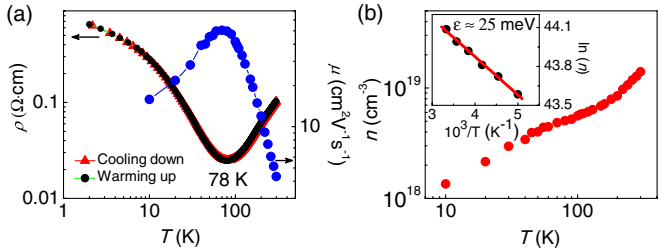

FIG. 2 (color online). (a) Temperature dependences of the resistivity (ρ-T) during different measurement processes and its carrier mobility over the temperature range 300–2 K, and (b) the corresponding carrier density n. The Arrhenius plot of ln(n) for the temperature range 300–200 K and the linear fitting are drawn in the inset of (b).

freeze-out phenomenon [9,21]; the density of donors (O_{vac} here) is low such that the donor level is separated from the bottom of the conduction band. Hence once the temperature decreases, most of the free electrons will shrink down to the lower donor level and get trapped.

The activation energy ϵ at high temperatures, fitted using $n \propto e^{(-\epsilon/k_B T)}$, is ~25 meV [inset of Fig. 2(b)], which is close to the RT thermal energy. Simply taking this value to characterize the energy interval between the donor level and the bottom of the conduction band, a band diagram of the $SrTiO_{3-x}$ film can be obtained as depicted in Fig. 3 on the basis of the PL emission peaks [Fig. 1(d)]. The defect levels (close to the valence band) of $SrTiO_{3-x}$ are consistent with [20]. The RT $\rho \approx 0.1\ \Omega$cm and $n \approx 1.4 \times 10^{19}\ \mathrm{cm}^{-3}$ of the $SrTiO_{3-x}$ film are, respectively, 30–50 times smaller and ~30 times larger than those of the bulk samples with the similar carrier freeze-out phenomenon [9]. These strongly suggest that the uniform area of the O_{vac} in a bulk $SrTiO_{3-x}$ is at most one-tenth of the whole single crystal thickness. So all the previous data of ρ and n [6–11] related to the bulk $SrTiO_{3-x}$ should be reconsidered carefully.

The corresponding carrier mobility (μ) from 300 to 10 K [Fig. 2(a)] is overall small and peaks around the phase transition temperature below which the mobility decreases with decreasing temperature due to the carrier freezing. At high temperatures, the linear power law dependence of μ on temperature is more obvious. The frozen state can be reexcited by larger electric fields at low temperatures. As shown in Fig. 4(a), ρ decreases with increasing measuring current especially below 10 K. At 2 K, ρ (obtained from dI/dV measurement) clearly displays a large negative electroresistance originating from the electrical excitation of the trapped electrons, which is defined as $[\rho(I) - \rho(0)]/\rho(0)$ and reaches −50% when the excitation current is 2 mA [inset of Fig. 4(a)]. Additionally, it was found that there is also a time dependence of ρ for the frozen state. As seen in Fig. 4(b), ρ at 2 K relaxes with the continuous measuring time, which suggests that the thermal effect is playing an important role. This is because the thermal conductivity of STO at low temperatures is very low [10] and it further decreases when oxygen content in the sample is reduced [22] due to the scattering of phonons from O_{vac}. Therefore the local temperature on the sample surface would increase as a result of the Joule heat accumulation, resulting in a decrease of ρ under the low temperature frozen nonmetallic state. However, the thermal effect at 2 K is much weaker than the electrical reexcitation.

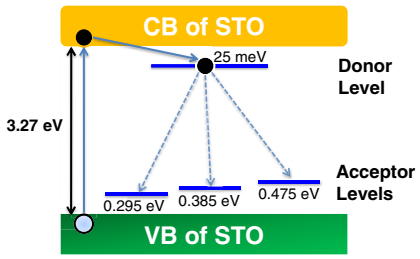

FIG. 3 (color online). Band diagram of the $SrTiO_{3-x}$ film and also the possible light emission mechanism. The energy intervals are not drawn to scale.

The 9 T magnetic field perpendicular to the sample surface results in a negative MR although it is relatively small and can only be seen below 5 K [Fig. 5(a)]. It was found that there was an asymmetry in the first curve obtained by scanning the field from −9 to 9 T. To check whether the asymmetry was due to an improper measurement geometry, the sample was warmed up to RT and then cooled down to 2 K. The measurement was then repeated by scanning the field from 9 to −9 T. It was found that there was always an asymmetry generated from an additional overall decrease in ρ over the measuring time regardless of the scanning sequence of magnetic field; this indicates that the asymmetry in the MR curves is from the thermal effect. The positive MR under small magnetic fields can be easily elucidated by the orbital scattering because the magnetic field was applied perpendicular to the current. The positive MR is very small because of the poor mobility in the frozen state. However, there should still be another mechanism competing with the orbital scattering to account for the negative MR. Because the resistance at low temperatures is predominantly from the trapping of carriers, the large magnetic field may physically detrap the localized electrons from the trapping centers with the assistance of an excitation electric field via the Lorentz force, resulting in a negative MR. On the other hand, O_{vac} in the TiO_2 interface layer can also enhance the tendency for ferromagnetism considerably [23] similar to the Ti 3d electrons from interface charge transfer [4,24], which may also be possible for the negative MR seen here.

The bulk STO single crystal, vacuum annealed together with the STO film, is metallic over the whole temperature range of 300–2 K. The quadratic MR at 2 K [Fig. 5(b)] is quite large up to ~900% at 5 T because of an extremely high mobility exceeding 10 000 $\mathrm{cm}^2\,\mathrm{V}^{-1}\,\mathrm{s}^{-1}$ [inset of

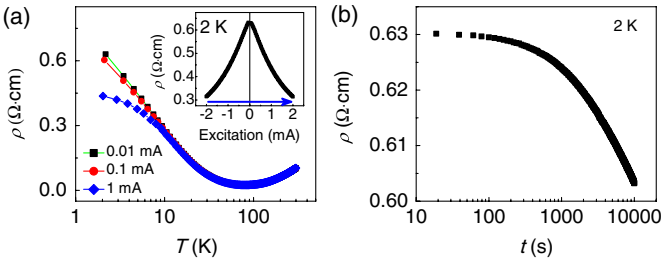

FIG. 4 (color online). (a) ρ-T curves of the $SrTiO_{3-x}$ film measured by the different currents, i.e., 0.01, 0.1 and 1 mA. (Inset) ρ at 2 K (obtained by the dI/dV measurement) versus the measuring current from −2 to 2 mA. (b) Time dependence of ρ at 2 K determined by 0.01 mA for a continues measurement up to 10 000 s.

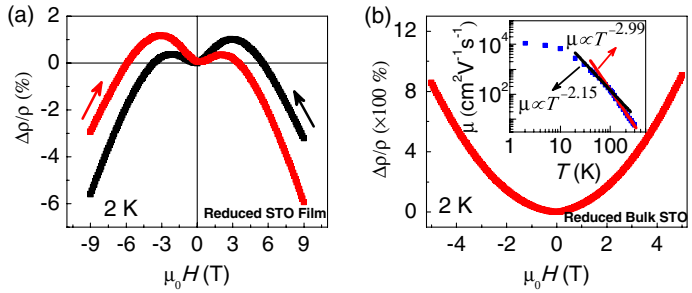

FIG. 5 (color online). (a) Out-of-plane magnetoresistance of the $SrTiO_{3-x}$ film up to 9 T and (b) the $SrTiO_{3-x}$ single crystal substrate up to 5 T which was vacuum-annealed together with the $SrTiO_{3-x}$ film. The temperature dependence of the carrier mobility for the latter is shown on a logarithmic scale in the inset of (b).

Fig. 5(b)] and does not show any signature of a negative MR up to 5 T. This strengthens the idea that the negative MR of the $SrTiO_{3-x}$ film is closely related to the carrier freezing state. Additionally, the bulk $SrTiO_{3-x}$ seems to be more conductive than the $SrTiO_{3-x}$ film since there is no carrier freeze-out in it. This evinces that the local concentration of O_{vac} in the bulk $SrTiO_{3-x}$ surface is larger than that in the $SrTiO_{3-x}$ film although they were reduced together, which strongly suggests that there is a sharp gradient in the concentration of O_{vac} in the bulk $SrTiO_{3-x}$ sample from the surface to inside. Thus all the electrical properties related phenomena in bulk $SrTiO_{3-x}$ should be mostly just the local properties of the near surface area.

Interestingly, the behavior of the carrier freeze-out observed here is quite comparable to the spin glass behavior [25,26], for example, the carrier freezing transition, the relaxation of the frozen ρ (although here is due to the thermal effect) and the suppression of the frozen state by the external fields. From this aspect, we can also coin this as "charge glass" to more vividly represent its characteristics.

In summary, we argued the uniformity of O_{vac} in the bulk $SrTiO_{3-x}$ single crystals by studying the high quality $SrTiO_{3-x}$ single crystal film via various means. It was found the actual uniform thickness of the bulk $SrTiO_{3-x}$ is around several 10 times smaller than the whole thickness and all the intriguing electrical phenomena of the bulk $SrTiO_{3-x}$ could only be the local surface properties due to the obvious gradient in the concentrations of O_{vac} from surface to inside. Moreover, we investigated the MIT observed in the $SrTiO_{3-x}$ film. The low temperature frozen state can be remarkably reexcited by the applied electric field. The thermal effect in $SrTiO_{3-x}$ film during the electrical measurements is pronounced owing to its poor thermal conductivity. It was also found that large external magnetic fields can suppress the carrier freezing and generate negative MR. The possible mechanism proposed for that is the magnetic field can detrap the localized electrons under the frozen state through Lorentz force with the help of an electric excitation. The high similarity between the various behaviors of the carrier freeze-out and the spin glass state enables us to think of the carrier freezing state as a kind of "charge glass" state.

We thank the National Research Foundation (NRF) Singapore under the Competitive Research Program (CRP) "Tailoring Oxide Electronics by Atomic Control" NRF2008NRF-CRP002-024, National University of Singapore (NUS) cross-faculty grant and FRC (ARF Grant No. R-144-000-278-112) for financial support.

*ariando@nus.edu.sg

[1] K. A. Müller and H. Burkard, Phys. Rev. B **19**, 3593 (1979).
[2] A. F. Santander-Syro *et al.*, Nature (London) **469**, 189 (2011).
[3] W. Meevasana *et al.*, Nature Mater. **10**, 114 (2011).
[4] Ariando *et al.*, Nature Commun. **2**, 188 (2011).
[5] K. van Benthem *et al.*, J. Appl. Phys. **90**, 6156 (2001).
[6] J. F. Schooley *et al.*, Phys. Rev. Lett. **12**, 474 (1964).
[7] J. F. Schooley *et al.*, Phys. Rev. Lett. **14**, 305 (1965).
[8] H. P. R. Frederikse *et al.*, Phys. Rev. **158**, 775 (1967).
[9] O. N. Tufte and P. W. Chapman, Phys. Rev. **155**, 796 (1967).
[10] H. P. R. Frederikse *et al.*, Phys. Rev. **134**, A442 (1964).
[11] C. S. Koonce *et al.*, Phys. Rev. **163**, 380 (1967).
[12] A. E. Paladino *et al.*, J. Phys. Chem. Solids **26**, 391 (1965).
[13] Ohtomo and H. Y. Hwang, Nature (London) **427**, 423 (2004).
[14] C. Herring, J. Appl. Phys. **31**, 1939 (1960).
[15] H. Fujisada *et al.*, Phys. Rev. B **3**, 3249 (1971).
[16] M. Imada *et al.*, Rev. Mod. Phys. **70**, 1039 (1998).
[17] M. Wöhlecke *et al.*, J. Appl. Phys. **48**, 1748 (1977).
[18] Y. Du *et al.*, Appl. Phys. A **76**, 1105 (2003).
[19] A. Dejneka *et al.*, Phys. Solid State **52**, 2082 (2010).
[20] D. Kan *et al.*, Nature Mater. **4**, 816 (2005).
[21] T. C. Harman *et al.*, Phys. Rev. **104**, 1562 (1956).
[22] C. Yu *et al.*, Appl. Phys. Lett. **92**, 191911 (2008).
[23] N. Pavlenko *et al.*, arXiv:1105.1163v1.
[24] A. Brinkman *et al.*, Nature Mater. **6**, 493 (2007).
[25] K. Binder and A. P. Young, Rev. Mod. Phys. **58**, 801 (1986).
[26] M. D. Mukadam *et al.*, J. Appl. Phys. **103**, 123902 (2008).